Direct Three-Dimensional Visualization and Characterization of Microstructures Formed by Printing Particles

Shu Chang, Vineeth R. Patil, Di Bai, and Marcos Esterman, Rochester Institute of Technology, Rochester, New York, USA

Abstract

Additive manufacturing performed with solid particles can form microscopic structures based on the properties of the particles used. These microstructures will likely impact the performance of the product produced. Characterizing these microstructures is difficult since the interior of powders is a challenge to image. Most imaging techniques are limited to surface visualizations.

We have established a methodology to directly visualize the resulting particle structure by mapping powder particle positions in the interior three-dimensionally. We use Confocal Laser Scanning Microscopy (CLSM) to capture stacks of cross-sectional images of micron-sized poly-dispersed electro-photographic printing particles. Assisted with image analysis tools, we have obtained the co-ordinates and deduced the radius for each particle in selected sampling volumes. With this information, we are able to recreate the particulate structure in three-dimensional space and to determine the microstructural parameters, such the packing fraction for this powder system.

Introduction

Micron-size particles have been used in numerous industries for a broad range of applications. One example is electrophotographic printing where polymeric particles have been the carrier of color pigments and the enabler for deposition and permanency of the pigments on substrates for the production of digital prints in graphic communication. Most recently the manufacturing world has adopted the graphic communication industry's digital printing processes, and consequently the use of micron and sub-micron particles.

The manufacturing adaptation of printing takes the form of adding materials to build parts, in contrast to the traditional subtractive process where materials are removed. Additive manufacturing, also known as functional printing or three-dimensional (3D) printing, has been advanced for the purpose of improving manufacturing capability in form (such as shape), fit (such as processes and tolerances), and function (such as high performance material systems). For powder-based additive manufacturing, similar to electrophotographic (EP) printing, the quality of a product will be influenced by particle structures resulting from the print process and materials used. For instance, a missing placement of a particle aggregate such as a halftone dot, will result in a missing "mark" in the manufactured product, which consequently leads to a defect in the product and a potential failure in its application.

Many micron-size powders are cohesive [1-3]. Cohesive particles will likely form highly porous structures [1, 2]. It has been demonstrated that the porosity of particle structures can directly impact the properties of images in electrophotographic printing [2, 3]. Visualizing particle microstructures can be difficult since it requires imaging the interior of powders. Much of the quantification of particle microstructures is through their packing fractions *(defined as the ratio of the volume occupied by solid particles to the total volume)* which can be estimated through inference from other measurements [1] or simulations [4, 5].

Visualization of microscopic structures has been limited to surface techniques, typically electron microscopies such as Scanning Electron Microscopy (SEM) [3, 6-9]. High Resolution SEM imaging of powder highlights the structures and voids on the surface within view [3, 6-9]. However, such reconstructions do not reflect the actual microstructures in the interior.

Confocal Laser Scanning Microscopy (CLSM) is a high-resolution optical microscope with depth selectivity and is capable of imaging interior structures for samples that are transparent or fluorescent. 3D imaging with CLSM has been conducted for 1-2 micron particles in colloidal systems to study the atomic nucleation process with dispersed mono-dispersed "hard spheres" [10-12]. Experimentation on these systems is performed with thin (a few layers of particles) and dilute samples for the transmission efficiency of light [13, 14]. The works on particle tracking in real space with the CLSM have yielded an unprecedented level of information on crystal nucleation [15] and phase transitions [11, 12]. The CLSM has also been employed for the studies of biological [16] systems. Included among the many CLSM applications for biological systems is the mapping of shape through the tracing of signals from fluorescence dyes that have been intentionally instituted on the surfaces of the sampling objects.

The goal of this research is to develop a methodology that is capable of identifying particle positions in the interior of a powder to illustrate and characterize the structure it forms. The methodology extends the Confocal Laser Scanning Microscopy (CLSM) to larger size and higher density powder systems. The methodology involves the capture of stacks (in the depth direction) of planar images of powder particles with CLSM and the analysis of the stacks of images through their pixelated values. Electrophotographic printing (EP) particles are used for the study because they possess the florescent property and because they have been characterized extensively in print quality studies [2, 3].

This work demonstrates the feasibility of using CLSM to three-dimensionally map and visualize interior structures of a particle sediment. This study will shed light to understand the performance of parts produced from additive manufacturing as well as characterize image quality in digital EP toner printing.

Methodology

In this study, yellow toners were employed which were extracted from an HP3700 cartridge. The particle sediments were created by simply dropping a small quantity of toner onto a microscope glass slide using a spatula. Samples of sediments were enclosed with double-sided tapes and another glass slide on top to prevent toner contamination of the CLSM imaging system. There are two reasons for utilizing sediments on glass slides instead of printed unfused samples on transparencies: (1) a desire to generate thick but image-able specimens to represent individual volumetric units resulting from additive manufacturing and (2) CLSM calls for

transparent substrates for the transmission of light. Transparencies used in digital printing scatter the laser beam and blur the images.

Imaging areas were then identified and within which individual sampling areas were magnified and stacks of XY images were collected. All sampling areas were approximately 44.5 µm x 44.5 µm in size to roughly simulate a 600 spots per inch printing addressability. Figure 1 illustrates this selection process of a sampling area. Figure 1 is a CLSM top view of an imaging area consisting of EP toner. From this area a sampling specimen, such as the region boxed by a square in the upper left quandary of the image, is selected for XYZ imaging. A stack of XY images is then attained sequentially in the perpendicular direction into this viewing surface (Z axis). For this study, stacks of cross-sectional images were collected for a total of nine sampling areas.

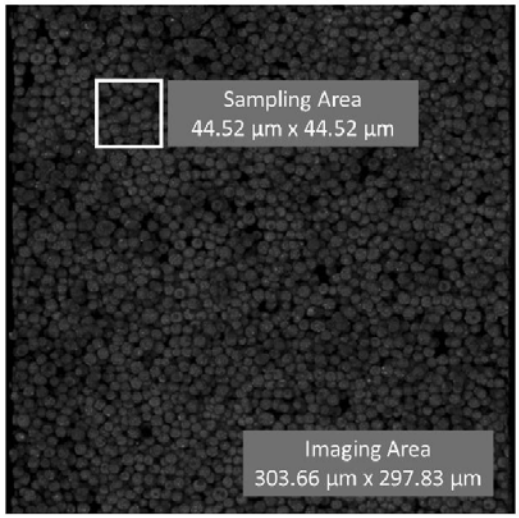

Figure 1. *Top image of an area of toner. The boxed area marked by white lines is selected to be sampled in Z-stack.*

The CLSM at Rochester Institute of Technology is a Leica TCS SP-5 Biological Confocal Microscope. For this study, the images were collected at a lateral frequency of approximately 0.05 µm x 0.05 µm. The Z axis sampling step was set to about 0.2 µm. The CLSM was imaged with a 40X objective with Numerical Aperture of 1.1 and with water as the refractive medium to interface the objective lens and the sample glass slide cover. The sample was imaged in the fluorescence mode with an excitation wavelength of 476 nm. The fluorescence emissions from the sample were collected in the 475 nm – 610 nm range. One XY image was obtained for each Z sampling step. XY images obtained at different Z increments were then stacked together with the stack covered the entire sample thickness. Images were stored in J-peg format for analysis.

Measurement

Once a stack of XY images have been collected for a specimen as defined above, each particle's coordinates and radius within the specimen are identified through a two-step process: (1) deduce XY coordinates and the radius for all particles in each of the cross-sectional plane and (2) repeat step 1 for the entire stack of images to determine when the particle's radius reaches a maximum and use the plane corresponding to maximal radius for the Z-position for each particle. We assume these particles to be spherical. We repeat this procedure for all particles in a selected sampling volume, such as the one marked by the white square box in fig. 1 and for all sampling areas studied.

1. Identify Particle's XY Coordinates and Radius

Figure 2 displays a cross-sectional plane from the sampling stack of a "boxed" area. At much higher magnification than fig. 1, fig. 2 identifies toner in grey areas (indicating fluorescence) through contrast against the black background (indicating no-fluorescence). The contrast marks out many grey-shade, approximately circular objects with different diameters.

In fig. 2, a particle has been marked by the white circle to be the "particle of interest" to illustrate the analysis performed. The marking of the circle was performed in MatLab using an 'imfindcircles' function with the 'Sensitivity Factor' of the function set to 0.95 and the 'Edge Gradient Threshold' to 0.1, both on a scale of 0 to 1. The 'Sensitivity Factor' is for the detection of circular objects. As the sensitivity factor increases, imfindcircles detects more circular objects, including weak and partially obscured circles. The 'Edge Gradient Threshold' is for determining edge pixels in the image, with '0' for zero-gradient magnitude and '1' for the maximum gradient magnitude. 'imfindcircles' detects more circular objects (with both weak and strong edges) when the threshold is at a low value. It detects fewer circles with weak edges at increasing value of threshold. The settings appears to be able to locate all particles within each cross-sectional image and are consistent with validations from manual measurements.

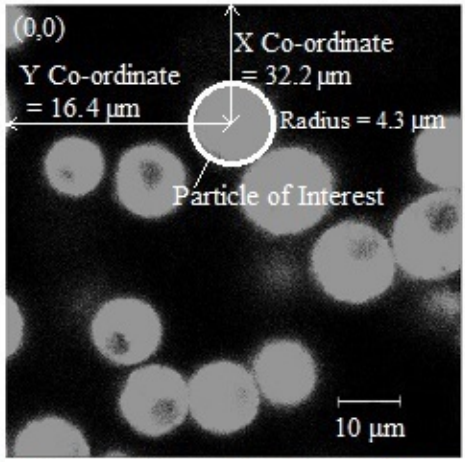

44.5 µm x 44.5 µm imaging area

Figure 2. *Image from one cross-sectional plane of the sampling area where a particle is selected as the Particle of Interest. For this particle, the X and Y co-ordinates are at 32.2 µm and 16.4 µm respectively and the radius is 4.3 µm.*

Also depicted in fig. 2 are the X coordinate, Y coordinate, and the radius identified by the 'imfindcircles' function for the "particle of interest". In the actual analysis, this action is automatically performed for all of the particles shown in fig. 2, thus obtaining X coordinates, Y coordinates, and the radii for all particles in view.

As the particles are situated at different height from the top surface of the receiving glass slide, the displayed size variation comes from particles with centers at different "Z-heights" (zero is the top surface of the glass-slide receiver) as well as from a distribution of particle diameters. Dark "cores" appears inside of some of the particles. The dark "cores" are indications of the presence of either hollows or a different material that is non-fluorescent within these particles. It is quite common for toners to incorporate more than one binder resin for the purpose of reducing the fixing/fusing temperature in EP printing [17].

Step 1 in the measurement attains the X, Y coordinates and the radii of the particles in the volume that corresponds to the entire stack of XY image planes.

2. *Identify Particle's Z-Coordinate*

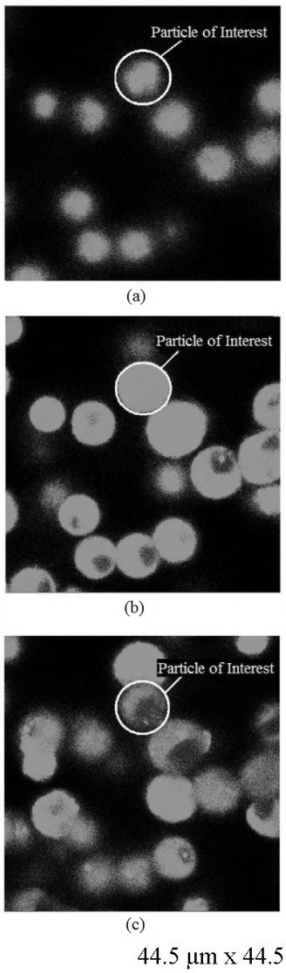

Figure 3*. Appearance of a "particle of interest" at three different image frames: a) at 4.0 μm, b) at 9.2 μm, and in c) at 13.0 μm. The radius of the particle is the largest in image B than those in images A and C.*

After step 1 has been performed for the entire stack of XY images, the radii measured from different planes for the particle are compared to identify a Z-plane that contained the maximal value. The Z position for the center of the particle is assigned to be the Z-value from the maximal radius plane. This is the method which we applied for the analysis. The Z position for a particular particle is also attainable through the maximum of the fluorescence intensity profile. However, this method is not selected here because of the dark "cores" aforementioned which obscure the true maximum in the intensity profile.

Figures 3 and 4 illustrate process to locate the maximal particle radius, therefore the Z-position, for the "particle of interest". Displayed in fig. 3 are cross-sectional images, A, B, and C, for the particle at three different depths or Z-planes. The dimensions of the image, or this volumetric unit, are 44.5 μm by 44.5 μm by 32.2 μm. The Z position for the "particle of interest" in fig. 3A is 4.0 μm, in fig. 3B is 9.2 μm, and in fig. 3C is 13.0 μm, with zero being the top surface of the receiving slide. The "particle of interest" is marked in all three images with the identical circles (white lines).

By comparison, the radius for the particle in fig. 3B is greater that the radii shown in figs. 3A and 3C for the same particle. As the size of a particle increases in the image stack, the number of fluorescing pixels increases, causing the particle to appear bigger and brighter. Beyond the center plane of the particle, the particle 'disappears' or blurs out of the image as the number of fluorescing pixels decreases.

Following a similar process, one can also observe other particles "appearing" or "disappearing" from each of the three views, revealing particles centered at various Z positions. The particle 'starts' from the frame when it appears in the XY cross-sectional image and 'ends' at the frame where the particle disappears in the image with variation of the depth. This method estimates the Z value for the center frame of the particle of interest at maximum radius.

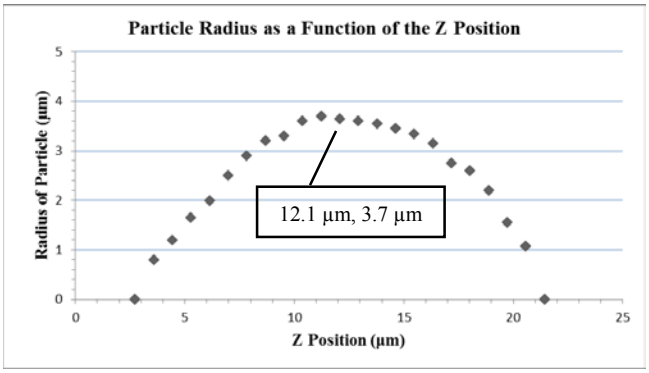

Figure 4. *Radius measured for a "particle of interest" from XY images as a function of the Z position for the cross-sectional plane. For this particle, the maximal radius determined from the XY plane is 3.7 μm and centered at 12.1 μm from the top surface of the receiving slide. The prolate spheroidal shape is caused by the three-dimensional diffraction pattern of light emitted from a small "point" source (toner in this case) in the sample [21].*

The change in the radius value for a "particle of interest" is plotted as a function of the Z-position for the cross-sectional plane in fig. 4. The maximal radius of about 3.7 μm occurs at a Z-position of approximately 12.1 μm. The correspondence of the particle radius with respect to the XY imaging plane position appear to indicate a prolate spherical shape for the particle, with the particle Z-dimension much larger than the radius in the XY plane. This appearance is caused by the three-dimensional diffraction pattern of light emitted from a small "point" source (toner in this case) [18, 19]. This effect is commonly observed and is referred to as the actual image convoluted with a "point spread function" [18, 19]. Although the effect causes elongation of the dimension, the center

position of the particle is not affected [19]. We have treated the particles as spherical with radii assuming values measured from the XY cross-sectional planes.

Step 2 in the measurement attains the Z coordinates for the particles in the volume that corresponds to the entire stack of XY image planes. This two-step measurement thus delivers the X, Y, and Z coordinates as well as the radii for the particles in the sampling specimens.

Analysis

There are a number of analyses that can be conducted with the measured X, Y, and Z values and the radii of particles. This paper presents the following:

1. Size Distribution

Using the two-step measurement described above, we obtained XYZ co-ordinates and radii in XY center planes for 126 toner particles in 9 samples. These particle sizes range from 1.8 µm to 5.4 µm. Analysis indicates that the particle sizes have a normal distribution with a mean radius of 3.6 µm and standard deviation of 0.7 µm. This is consistent with SEM measurement of sizes for the same particles [20].

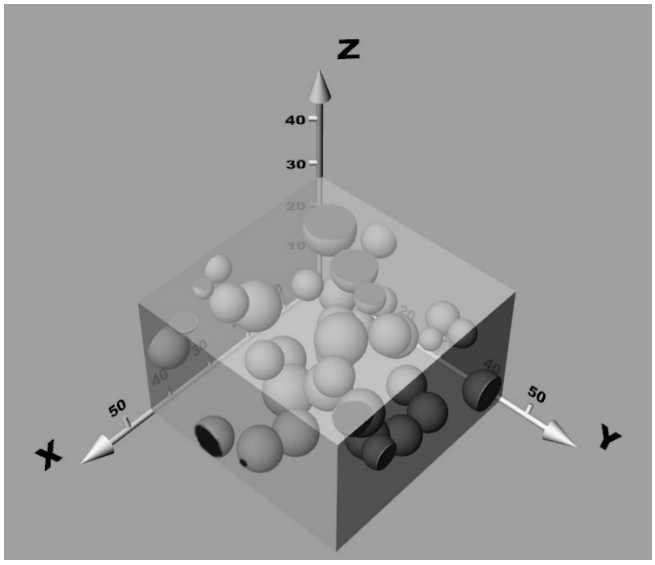

Figure 5*. Reconstruction of particles in a volumetric unit of 44.5 µm x 44.5 µm x 27.2 µm in size. The "suspended" particles are in actual contacts with and being supported by particles in the neighboring volume cells.*

We can reconstruct the particles in a volumetric unit in 3D space. Figure 5 shows such a reconstruction. There are 25 full and 13 partial particles in the 44.5 µm x 44.5 µm x 27.2 µm volumetric units shown in fig. 5. Figure 5 depicts the larger particle size range, reflecting the polydispersive nature of toner. The particles in this volume space have a mean radius of 3.5 µm and a standard deviation of 0.7 µm.

2. Reconstruction of the Particle Structure

Figure 5 re-creates the geometric structure formed by toner particles. Previous work has simulated EP toner deposition process using a Random Ballistic Deposition process model [2]. The simulation demonstrated that for toner, or "sticky" particles, the deposition results in a loosely packed structure that resembles dendritic tentacles. The reconstruction in fig. 5 illustrates openness in the particle structure with very high porosity. This openness in fig. 5 resembles those projected by simulations for cohesive, or "sticky" particles [2, 4, 5]. Figure 5 displays several particles appearing "suspended" in space. These particles are in fact in contact with and supported by particles in the neighboring volume units.

3. Particle Structure Characterization

The particle measurement will enable characterizations for particle morphology. One parameter that has been widely used to describe structures formed in powder materials if the packing fraction. A packing fraction is defined as the ratio of the volume occupied by solid particles in a volumetric cell to the total volume of the cell. A packing fraction is the complement of porosity, which is the ratio of open space that is not occupied by the particles in a volumetric cell to the total volume of the cell. Packing fractions have been generally deduced from other forms of measurements [2, 3, 5].

The study here enables directly estimation from the participating particles. The total volume occupied by the particles within the volumetric unit can be summed up from each particle within the sampling cell and each partial particle on the cell surfaces, edges and corners. This total volume of the particles within the cell, denoted Vp, can be calculated from:

$$Vp = \sum_i Vi(interior) + \sum_j Vj(surfaces) + \sum_k Vk(edges) + \sum_l Vl(corners) \quad (1)$$

Where i = number of particles in the interior, j = number of partial particles residing on the 6 surfaces and excluding those on the edges and at the corners, k = number of partial particles on the 12 edges and excluding those at the corners, and l = number of partial particles at the 8 corners, all within the rectangular cube of w (width), h (height), and d (depth).

The packing fraction of the particle structure, denoted as Φ, is then:

$$\Phi = \frac{Vp}{Vc} = \frac{Vp}{w \times h \times d} \quad (2)$$

Theoretical simulations of Random Ballistic Deposition of cohesive particles predict a packing fraction of about 14.7% [2, 5]. Estimation from the particle measurement here has resulted in 13.9% ± 1.5% packing fraction for the 9 samples examined. Comparable values between the result from this study and the predictions from simulations in the literature indicate that EP toners are indeed cohesive with particle structures similar to that of the random ballistic deposition of cohesive particles.

The cell in Figure 5 has an estimated packing fraction of 13.21 %.

Conclusion

We have demonstrated the feasibility of a methodology that is capable of identifying particle positions in the interior of a powder, of creating visualization of the particle microstructure, and of characterizing the microstructure that the particles form. Using the Confocal Laser Scanning Microscopy and image analysis tools, we have obtained the X, Y and Z co-ordinates of the EP toner particles in a sediment state. We have obtained particle sizes and the particle size distribution. We have further employed this information to reconstruct a particle volume cell.

This mapping and reconstruction of particles in 3D space demonstrates the feasibility to visualize powder interiors and to characterize quantitatively the microscopic structures. We have used the particle packing fraction to illustrate how property of powder materials can be quantified. This research has successfully achieved its goal and underscores a unique possibility to make significant progress in the understanding of the structure-property relationship for powder materials.

Acknowledgements

This research is supported by the Melbert B. Cary Jr. endowment by the College of Imaging Arts and Science and the Cross-Media Innovation Center at Rochester Institute of Technology as well as by the National Science Foundation Partnerships for Innovation Building Innovation Capacity (PFI: BIC) subprogram under Grant No. 1237761. Any opinions, findings, and conclusions or recommendations expressed in this material are those of the author(s) and do not necessarily reflect the views of the National Science Foundation. The RIT Confocal Laser Scanning Microscopy lab is supported through the National Science Foundation Major Research Instrumentation Program (#1126629), the RIT Office of the Vice President for Research, Kate Gleason College of Engineering, and the RIT College of Science. The authors wish to thank Dr. Cheryl Hanzlik for the guidance provided for the Confocal Laser Scanning Microscope.

References

[1] J. Blum and R. Schrapler, Structure and Mechanical Properties of High-Porosity Macroscopic Agglomerates Formed by Random Ballistic Deposition, Phys. Rev. Lett., 93 (11), 1155031-1155034 (2004).

[2] H. Mizes, The Structure of Toner Sediments Simulated with Random Ballistic Deposition, Ima. Sci. & Tech. Florida USA, 15, 495-498 (1999).

[3] S. Chang, H. Till, E. Viturro, K. Watson, A. T. Perez, A. Gonzalez and A. Castellanos, Measurement of Toner Cohesion in Liquid Inks Using a Visualization Cell, Ima. Sci. & Tech. Toronto Canada, 218-221 (1998).

[4] J. Zhou, Y. Zhang, and J. K. Chen, Numerical Simulation of Random Packing of Spherical Particles for Powder-Based Additive Manufacturing, *J. Manuf. Sci. Eng.,* 131, 031004-031004 (2009).

[5] J. M. Valverde, and A. Castellanos, Random loose packing of cohesive granular materials, Europhys. Lett., 75, 985 (2006).

[6] L. E. Murr, S. M. Gaytan, D. A. Ramirez, E. Martinez, J. Hernandez, K. N. Amato, P. W. Shindo, F. R. Medina, and R. B. Wicker, Metal Fabrication by Additive Manufacturing Using Laser and Electron Beam Melting Technologies, J. Mater. Sci. & Tech., 28, 1–14 (2012).

[7] D. A. Ramirez, L. E. Murr, E. Martinez, D. H. Hernandez, J. L. Martinez, B. I. Machado, F. Medina, and R. B. Wicker, Novel precipitate–microstructural architecture developed in the fabrication of solid copper components by additive manufacturing using electron beam melting, Acta Mater., 59, 4088–4099 (2011).

[8] L. E. Murr, S. A. Quinones, S. M. Gaytan, M. I. Lopez, A. Rodela, E. Y. Martinez, D. H. Hernandez, E. Martinez, F. Medina, and R. B. Wicker, Microstructure and mechanical behavior of Ti–6Al–4V produced by rapid-layer manufacturing, for biomedical applications, J. Mech. Behav. Biomed. Mater., 2, 20–32 (2009).

[9] K. N. Amato, S. M. Gaytan, L. E. Murr, E. Martinez, P. W. Shindo, J. Hernandez, S. Collins, and F. Medina, Microstructures and mechanical behavior of Inconel 718 fabricated by selective laser melting, Acta Mater., 60, 2229–2239 (2012).

[10] W. C. K. Poon, E. R. Weeks, and C. P. Royall, On measuring colloidal volume fractions, Soft Matter, 8, 21-30 (2012).

[11] A. D. Dinsmore, E. R. Weeks, V. Prasad, A. C. Levitt, and D. A. Weitz, Three-dimensional confocal microscopy of colloids, Appl. Opt., 40, 4152-4159 (2001).

[12] V. Prasad, D. Semwogerere, and E. R. Weeks, Confocal microscopy of colloids, J. Phys.: Cond. Mat., 19 1-25 (2007).

[13] C. P. Royall, W. C. K. Poon, and E. R. Weeks, In search of colloidal hard spheres, Soft Matter, 9, 17-27 (2013).

[14] P. Schall, I. Cohen, D. A. Weitz, and F. Spaepen, Visualization of Dislocation Dynamics in Colloidal Crystals, Science, 305.5692, 1944-1948 (2004).

[15] J. B. Jones, D. I. Wimpenny, R. Chudasama, and G. J. Gibbons, Printed Circuit Boards by Selective Deposition and Processing, Nanoscale, 22, 23 (2011).

[16] J. B. Pawley and B. R. Masters, Handbook of Biological Confocal Microscopy, Third Edition vol. 13: International Society for Optics and Photonics, 2008.

[17] S. Matsunaga, M. Ohno, T. Onuma, M. Shimojo, and C. K. Kaisha, Toner with wax component for developing electrostatic image, *Pat. US 5605778 A* (1997).

[18] M. C. Jenkins, and S. U. Egelhaaf, Confocal microscopy of colloidal particles: Towards reliable, optimum coordinates, *Adv. Col. & Int. Sci.*, 136, 65-92 (2008).

[19] R. W. Cole, T. Jinadasa, and A. M. Brown, Measuring and interpretting point spread functions to determine confocal microscope resolution and ensure quality control, *Nature Protocol*, 6 (12), 1929-1941 (2011).

[20] D. Bai and S. Chang, unpublished data (2014).

Author Biography

Dr. Shu Chang holds the Cary Distinguished Professorship in the College of Imaging Arts and Sciences. Her research identifies techniques to bridge different aspects of conventional digital printing to the rapidly growing field of print as a manufacturing process. Prior to joining RIT, She worked at Xerox Innovation Group in Webster New York, where her work spanned from printing technologies and materials science research to sustainability in printing. Dr. Chang obtained her Ph.D. in Materials Science from the University of Minnesota.

Vineeth Patil is a graduate student in Materials Science and Engineering at RIT. Vineeth is working on his Master's Thesis under the guidance of Dr. Shu Chang and Dr. Marcos Esterman on simulating and imaging of structures formed by printing particles.

Di Bai is a graduate student of RIT majoring in Print Media. He received his bachelor degree of print engineering from Wuhan University, China. Di is working on his Master's Thesis under the guidance of Dr. Shu Chang on imaging, reconstructing, and characterizing the structures formed by printing particles three-dimensionally.

Dr. Marcos Esterman is an Associate Professor in the Industrial and Systems Engineering Department at RIT. He focuses on structured product development methods, sustainable printing and print as a manufacturing process. Prior to joining the RIT faculty, he worked for Hewlett-Packard's Imaging and Printing Division in Boise, Idaho. His work at HP enhanced

design and product architecture decision-making. Dr. Esterman holds BS and MS degrees from MIT and a PhD from Stanford University, all in Mechanical Engineering.